THE SÃO PAULO MICROTRON RESEARCH PLANS

M. N. Martins, N. L. Maidana, V. R. Vanin

Laboratório do Acelerador Linear
Instituto de Física da Universidade de São Paulo, CP 66318, 05315-970 São Paulo, SP, Brazil, martins@if.usp.br

The Linear Accelerator Laboratory (LAL) of the Instituto de Física da Universidade de São Paulo (IFUSP) is building a two-stage racetrack microtron, which will generate continuous wave electron beams with energies up to 38 MeV. This paper describes the characteristics of the accelerator, and reports on the experimental equipment that will be available in order to pursue the photonuclear physics research program. Operation will begin with the first stage (5 MeV), and concentrate on NRF (Nuclear Resonance Fluorescence) measurements and radiation physics studies. Planned experiments for the second stage explore the cw character of the beam on coincidence experiments. A photon tagger has been already tested with radioactive sources and is ready to be installed. Gamma and neutron detector arrays are being developed for the detailed study of photoneutron reactions. Plans include the study of NRF and pygmy resonances, near the neutron binding energy.

I. INTRODUCTION

The Linear Accelerator Laboratory (LAL) of the Instituto de Física da Universidade de São Paulo (IFUSP) is building a two-stage racetrack microtron, which will generate continuous wave electron beams with energies up to 38 MeV[ref.1,2]. Operation will begin with the first stage (5 MeV).

The accelerator comprises a 1.8 MeV injector linac, a five-turn microtron booster that increases the energy to 4.9 MeV, and the main microtron, which will be able to deliver a 38 MeV cw electron beam after 40 turns. The injector consists of a 100 keV electron gun, chopping and bunching systems, a capture section and a pre-accelerating section; therefore the complete accelerator has four RF accelerating structures, operating at 2450 MHz. This cascaded configuration was adopted in order to maximize the final energy of the system while keeping the RF power under 45 kW, so that the whole system could be powered with a single RF source, namely a 50 kW cw klystron, to minimize costs. Table I summarizes the characteristics of the accelerator.

TABLE I. Characteristics of the IFUSP microtron.

Electron gun	
Energy	100 keV (±0.1%)
Current	2 mA
Beam diameter	2 mm
Injector	
Input energy	0.1 MeV
Output energy	1.8 MeV
Booster	
Input energy	1.8 MeV
Output energy	4.9 MeV
Maximum current	50 μA
Number of turns	5
Main microtron	
Input energy	4.9 MeV
Maximum output energy	38 MeV
Maximum current	50 μA
Number of turns	40

The experimental hall, with two beam lines, is located 2.7 m below the accelerator room. One of the beam lines will be dedicated to experiments using tagged photons, and the other line will be used for high beam intensity experiments or production of X-rays by coherent bremsstrahlung[3]. Fig. 1 shows an isometric view of the machine in the accelerator building.

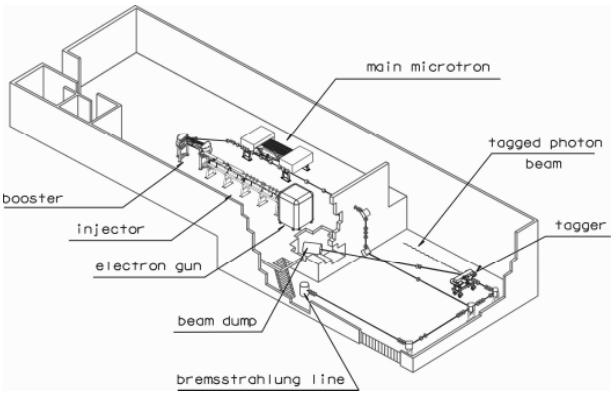

Fig. 1. Isometric view of the accelerator in the accelerator building.

II. EXPERIMENTAL PERSPECTIVES

The experiments intended to be done with the first stage – 5 MeV – are restricted to the study of nuclear bound states, using the nuclear resonance fluorescence (NRF) technique, and radiation physics experiments: optical transition radiation for beam monitoring purposes, and detailed study of energy deposition of electrons in crystals, in order to improve our knowledge of processes in HPGe gamma-ray detectors. The plans for the second stage – 38 MeV maximum energy – include a broader study of photonuclear reactions.

II.A. Nuclear Resonance Fluorescence

The experimental setup needed for NRF measurements is very simple and is sketched in Fig. 2.

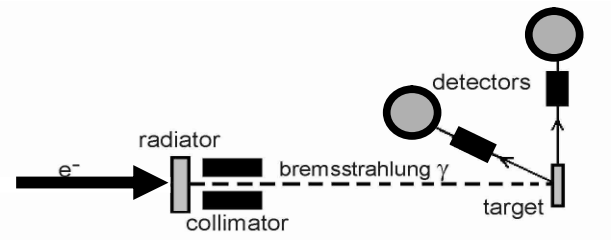

Fig. 2. Experimental setup for NRF measurements. The electron beam hits the radiator, producing a bremsstrahlung photon beam. After collimation, the photon beam hits the target, and the scattered radiation is detected by the HPGe detectors.

This kind of experiment allows for the possibility of level excitation-energy and electromagnetic transition multipolarity measurements; hence, the spin of the excited nuclear state, at least for even-even nuclei, can be determined. The cross section is obtained from the analysis of the spectra of scattered photons, and allows to measure the decay width to the ground state and, thus, in a model independent way, the reduced transition probability, $B(E\lambda/M\lambda)$.

II.B. Photonuclear Reactions

The cw beam from the microtron will allow the use of a photon tagger to produce monochromatic photons in the energy range between 3 and 35 MeV. The use of high duty cycle electron accelerators, combined to modern detector systems (like high solid angle charged particle or fission fragment detectors, and high resolution γ-spectrometers and polarimeters for photons), will open new possibilities both in photonuclear reactions and in nuclear spectroscopy, two areas where the LAL has scientific tradition.

The use of the photon tagger also opens the possibility of working with linearly polarized photons. Low energy monochromatic photons (linearly polarized or not) can produce interesting results in the photodisintegration of light nuclei as well as in studies of photofission at energies close to the fission barrier. The study of GDR properties by means of the experimental determination of its decay modes, measuring spectral and angular distributions of the emitted particles, presents great interest to the theoretical description of these processes.

Neutron detection is possible only by means of nuclear reactions. We plan to use thin plastic scintillators, lightly shielded with lead to reduce photon background and so avoid excessive dead time from the detection of photons. Neutron and photon signals will be discriminated by pulse shape analysis. Besides plastic scintillators, we will also use HPGe detectors, which are sensitive to neutrons above ~600 keV[ref.4,5]. HPGe crystals can be applied to detect neutrons due to their large active volume (about 150 cm^3), which allows for high efficiency. Preliminary tests with detectors available at the lab showed intrinsic efficiency of ~10%, taking into account only those events within a resolution time of 10 ns. The experimental setup is shown in Fig. 3. The detectors have their symmetry axes converging to the center of the target, forming different angles with the beam direction. To reduce the contribution from positron annihilation photons, detectors are placed avoiding 180^o separation among any pair. Although HPGe detectors can be damaged by neutrons, the reaction cross-section combined with the relatively weak tagged-photon flux results in a low neutron fluence that will not damage a mid-sized n-type detector (30-35% efficiency) before years of continuous use.

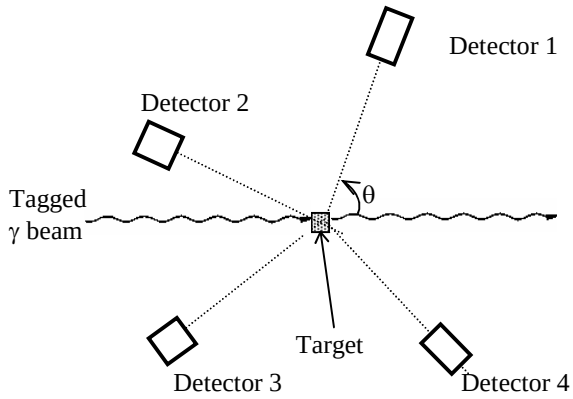

Fig. 3. Experimental setup for the detection of photons and neutrons.

Photodisintegration can be a powerful tool in the study of cluster properties of light nuclei. The cross section of the $\gamma + {}^7Li \rightarrow \alpha + t$ reaction, for instance, presents several interesting features that can be explored with the combination of instruments we are setting up at

the LAL. Several experiments and theoretical considerations show that ^{7}Li presents an α-t configuration[6-11]. The available ^{7}Li(γ,t)α cross section data in the literature present an inconsistent picture, as shown in Fig. 4. Measurements were done using virtual photons from electrodisintegration (continuous spectrum[12]), or bremsstrahlung photons (continuous spectra[13,14]). Results obtained with virtual photons are quite above those obtained with real photons, which do not agree with each other.

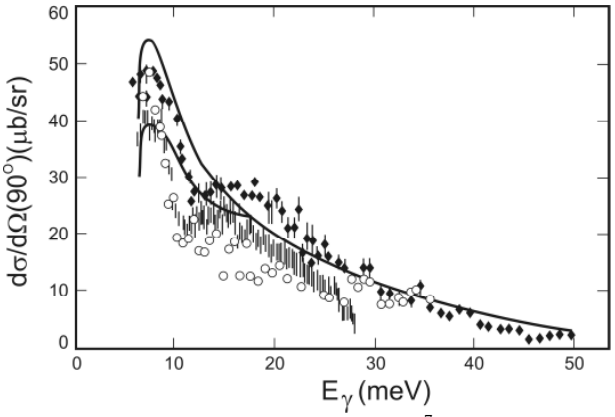

Fig. 4. Differential cross section for the ^{7}Li(γ,t)α reaction. Experimental results are represented by diamonds[13] (virtual photons), open circles[14] and vertical bars[15] (bremsstrahlung). The lines give results of calculations[15] with different potential depths in the α-t model.

II.C. Radiation Physics

To be prepared for planned NRF and photonuclear experiments, we are studying the response function of HPGe detectors to high energy photons ($E_\gamma > 6$ MeV) as well as to neutrons. Besides the actual measurements, the response function is being simulated using MCNP-5 and -X codes, and, in collaboration with J. Fernandez-Varea and L. Brualla (from Barcelona, Spain), the Penelope code. Fig. 5 shows a spectrum dominated by the interaction of 10.7 MeV photons with the detector, obtained in the reaction ^{27}Al(p,γ), with 992 keV protons from the Pelletron tandem accelerator at the LAMFI laboratory.

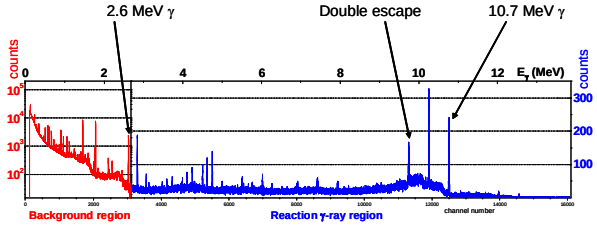

Fig. 5. Spectrum of photons from the ^{27}Al(p,γ) reaction, detected with a HPGe detector[16].

Besides the calibration of HPGe detectors for high energy photons, we are also studying their use as neutron detectors. Fig. 6 shows a spectrum from an AmBe source (10^5 neutrons/s), obtained in a 2.1-h long measurement with a HPGe detector placed 25 cm from the source. The neutron peaks from the reactions ^{72}Ge($n,n'e^-$) (692 keV) and ^{74}Ge($n,n'\gamma$) (598 keV) are clearly seen as broad, asymmetric peaks. Issues related to neutron energy determination and cross sections involved are still being studied.

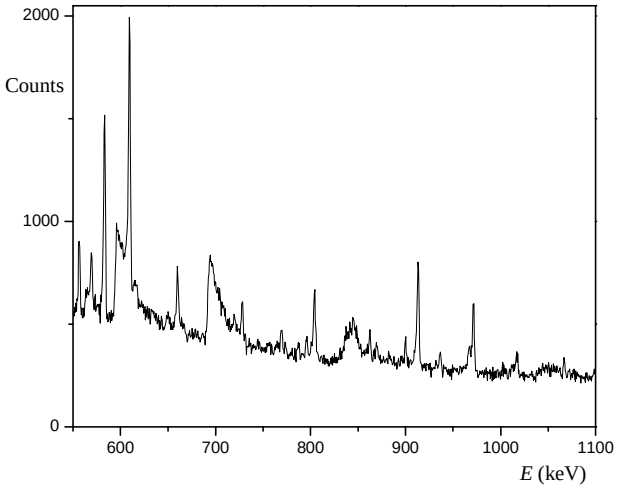

Fig. 6. HPGe spectrum of a AmBe source. The neutron events give rise to the broad, right-tailed peaks, observed at 598; 692; 834, and 1039 keV.

II.D. Experimental Equipment

The LAL is setting up a combination of instruments to fully use the characteristics of the cw beam from the São Paulo Microtron. This combination will comprise the photon tagger (given by the MAX-Lab, Lund, Sweden[17]), a scattering chamber with silicon strip detectors for charged particles[18], and high resolution HPGe photon detectors. A schematic drawing of the photon tagger is shown in Fig. 7.

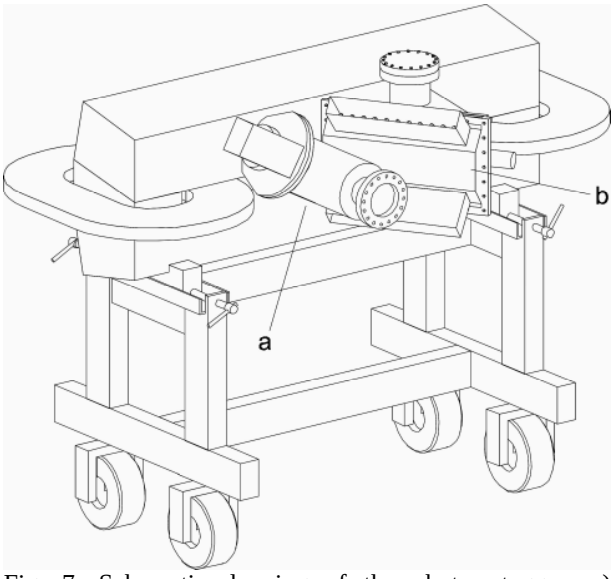

Fig. 7. Schematic drawing of the photon tagger: a) indicates the bremsstrahlung target chamber, and b) the focal plane vacuum chamber. All vacuum chambers are connected without windows.

The vacuum chamber, shown in Fig. 8, houses the silicon strip detectors and a target ladder that holds two targets and a radioactive alpha source for calibration.

Fig. 8. Vacuum chamber with silicon strip detectors for charged particle detection.

The silicon strip detectors are arranged in a geometry, depicted in the scheme of Fig. 9, which allows for: good energy resolution for heavy charged particles; good angular resolution; time resolution comparable to the difference in the time of flight of the particles; stability over large periods of time; possibility of illuminating a large target area; detector array as close as possible to the target. This arrangement is particularly suited for experiments involving very low cross sections.

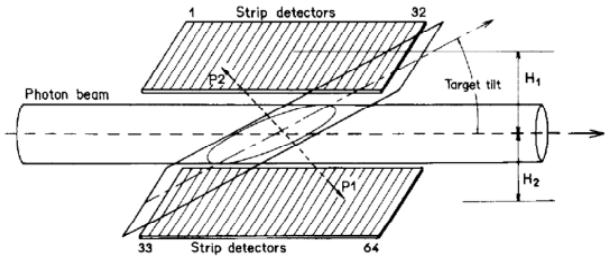

Fig. 9. Schematic drawing of the strip detector arrangement with a thin target.

This detector arrangement was designed for the specific case in which two reaction products are emitted in opposite directions (requiring a thin, self-supported target). For this reason, we opted to have a sandwich configuration where the target is tilted with respect to the photon beam and lies between two planes of detectors. The associated electronics, shown in the scheme of Fig. 10, selects any pair of opposing strips, thus determining the fragment emitted angles.

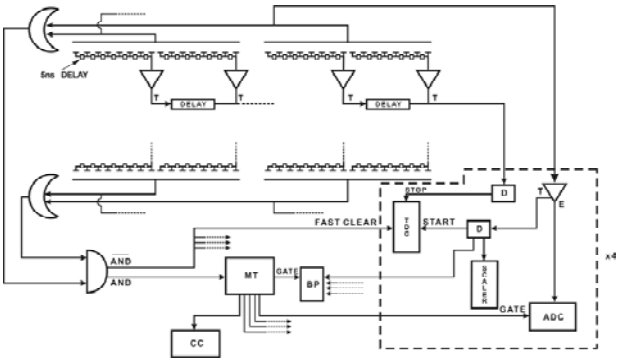

Fig. 10. The electronics setup. PA: preamplifier: D: discriminator; ADC: analog to digital converter; TDC: time to digital converter; CC: crate controller; BP: bit pattern; MT: master trigger. The dashed box depicts the electronics for one detector and is the same for all four detectors used.

III. CONCLUSIONS

We are setting up a facility that will be able to produce tagged photons in the range 3 to 35 MeV, and to measure photons, neutrons, and charged particles. This will be a very favorable setup to study photonuclear reactions in the giant resonance region, as well as low-energy nuclear physics subjects, like pygmy dipole resonances and nuclear resonance fluorescence.

ACKNOWLEDGMENTS

Work supported in part by FAPESP and CNPq.

REFERENCES

1. J. TAKAHASHI *et al.*, in *Proceedings of the EPAC92, Third European Particle Accelerator Conference*, 1992, edited by H. Henke (Editions Frontieres, Gif sur Yvette, France, 1992), p. 429.
2. J. TAKAHASHI *et al.*, in *Proceedings of the PAC97, Particle Accelerator Conference*, Vancouver, Canada, 12-16 May, 1997, p. 2998 (1997).
3. V. B. GAVRIKOV, V. P. LIKHACHEV, M. N. MARTINS, V.A. ROMANOV, Braz. J. Phys. 29, 516-523 (1999).
4. G. FEHRENBACHER, H.G. PARETZKE, R. MECKBACH, Nucl. Instr. Meth A**372**, 239 (1996).
5. A.J. PEURRUNG, Nucl. Instr. Meth A**443**, 400 (2000).
6. D. RYCKBOSCH *et al*., Nucl. Phys. A**568**, 52 (1994).
7. S. FRULLANI *et al*., 4th Workshop on Perspectives in Nuclear Physics at Intermediate Energies, ICTP, Trieste, Italy, 1989.
8. S. COSTA *et al*., Phys. Lett. **4**, 308 (1963).
9. V. I. KUKULIN *et al*., Nucl. Phys. A**417**, 128 (1984).
10. N. A. BURKOVA *et al*., Phys. Lett. B**223**, 136 (1989).
11. N. A. BURKOVA, M. A. ZHUSUPOV and R. A. M. ERAMZHYAN, Academy of Sciences of the USSR, Institute for Nuclear Research Preprint 702 (1991).
12. D. M. SKOPIK *et al.*, Phys. Rev. C**20**, 2025 (1979).
13. V. P. DENISOV and I. Ya. CHUBUKOV, Sov. J. Nucl. Phys. **35**, 11 (1982).
14. G. JUNGHANS, K. BANGERT, U. E. P. BERG, R. STOCK and K. WIENHARD, Z. Phys. A**291**, 353 (1979).
15. N. A. BURKOVA, *et al.*, Nucl. Phys. A**586**, 293 (1995).
16. CESAR OLIVEIRA GUIMARAES, *Eficiência de detetores HPGe para fótons de 4 a 10 MeV*, M.Sc Thesis, www.teses.usp.br, last accessed July 25, 2007.
17. J.-O. ADLER, B.-E. ANDERSSON, K. I. BLOMQVIST, B. FORKMAN, K. HANSEN, L. ISAKSSON, K. LINDGREN, D. NILSSON, A. SANDELL, B. SCHRÖDER and K. ZIAKAS, Nucl. Instr. and Meth, A**294**, 15 (1990).
18. V. P. LIKHACHEV, J. F. DIAS, M.-L. YONEAMA, M. N. MARTINS, J. D. T. ARRUDA-NETO, C. C. BUENO, V. PEREVERTAILO, O. FROLOV, Nucl. Instr. and Meth, A**376**, 455 (1996).